



Cite this: DOI: 10.1039/d3ew00043e

Impact of the surface aging of potable water plastic pipes on their lead deposition characteristics†

Md Hadiuzzaman,^a David A. Ladner ^b and Maryam Salehi ^{*c}

The use of plastic potable water pipes to replace corroded metallic plumbing and construct new potable water plumbing systems is rapidly increasing due to the low cost, noncorrosive characteristics, and easy installation of plastic water pipes. However, unlike for metallic pipes, the understanding of the fate of heavy metals within plastic potable water pipes is limited. This study elucidates the effect of plastic pipe surface aging on lead (Pb) deposition under stagnant conditions. Accelerated aging of crosslinked polyethylene-A (PEX-A) and high-density polyethylene (HDPE) pipes was conducted through exposure to a concentrated chlorine solution at an elevated temperature. Variations in the surface chemistry of the plastic pipes due to aging were examined *via* attenuated total reflectance-Fourier transform infrared spectroscopy (ATR-FTIR) and X-ray photoelectron spectroscopy (XPS) analysis. The kinetics of Pb deposition onto new and aged pipes were studied through 5 day Pb exposure experiments. Moreover, the influence of the initial Pb concentration [50–1000 $\mu\text{g L}^{-1}$] on the rate of Pb deposition onto the plastic pipes was investigated. The ATR-FTIR and XPS analysis revealed the formation of several oxidized carbon functional groups [$>\text{C}-\text{O}$, $>\text{C}=\text{O}$, $>\text{O}-\text{C}=\text{O}$] on the PEX-A pipe and HDPE pipe surfaces after 14 days of accelerated aging. Zeta potential measurements conducted on the HDPE pipes showed a slightly more negative surface charge for the aged pipes than for the new pipes. Kinetics experiments showed that the aged PEX-A (387 $\mu\text{g m}^{-2}$) and HDPE (418 $\mu\text{g m}^{-2}$) pipes deposited significantly greater levels of Pb compared to the new PEX-A (288 $\mu\text{g m}^{-2}$) and HDPE (335 $\mu\text{g m}^{-2}$) pipes at equilibrium. Pb deposition onto the new and aged PEX-A and HDPE pipes followed a first-order kinetics model implying surface confinement of the Pb species. As the initial Pb concentration was increased, a significantly greater rate of Pb deposition (p -value < 0.05) was found for aged PEX-A compared to new PEX-A. However, for new and aged HDPE pipes this rate was not significantly different (p -value > 0.05). This study provides the groundwork for future investigations into the fate of heavy metals in potable water infrastructure.

Received 24th January 2023,
Accepted 14th July 2023

DOI: 10.1039/d3ew00043e
rsc.li/es-water

Water impact

This research investigated the role of surface aging in lead deposition onto the surfaces of plastic potable water plumbing pipes. Studying the surface chemistry variations of crosslinked polyethylene and high density polyethylene pipes revealed the formation of several oxidized carbon functional groups due to the aging process. These oxidized carbon functional groups promoted lead surface accumulation. This study will inform water consumers, drinking water providers, and the public health sector regarding the potential risk of plastic pipes as a resting site for lead, which later, due to water chemistry fluctuation, might be released into the tap water.

Introduction

In the U.S., plastic pipes and fittings have been used in water distribution networks for more than 60 years. In new construction and renovations, metallic pipes are often replaced with plastic pipes that are lightweight, inexpensive, and easy to install, and do not face corrosion problems.¹ Polyethylene (PE) and polyvinyl chloride (PVC) comprise more than 90% of the plastic materials used for water distribution systems.² Crosslinked polyethylene (PEX) and high-density

^a Department of Civil Engineering, The University of Memphis, Memphis, TN, USA

^b Department of Environmental Engineering and Earth Sciences, Clemson University, Anderson, SC, USA

^c Department of Civil and Environmental Engineering, University of Missouri, Columbia, MO, USA. E-mail: mshfp@missouri.edu, msalehiesf@gmail.com

† Electronic supplementary information (ESI) available. See DOI: <https://doi.org/10.1039/d3ew00043e>

Polyethylene (HDPE) pipes are being primarily installed for building potable water plumbing systems and service line connections.³ Among the three types of commercially available PEX pipes [PEX-A, PEX-B, PEX-C], types A and B are more commonly used for drinking water plumbing systems. The PEX pipe installation rate has increased from 7% in 2001 (ref. 4) to 54% for renovations and 75% for new building construction in 2013.⁵ On the other hand, utilization of HDPE pipes for new building construction has been estimated to be 13%, a figure which was doubled during the last decade.²

Although plastic potable water pipes are not prone to corrosion, they may undergo chemical aging when they are used to convey disinfected drinking water. Free chlorine (Cl_2) and chlorine dioxide (ClO_2) are two strong oxidants used to disinfect drinking water. Moreover, chloramine is a widely used disinfectant that is more stable and has a longer-lasting residual effect compared to free chlorine.⁶ Previous studies demonstrated that disinfectant residues present within the tap water could attack and oxidize PEX pipes.⁷⁻⁹ Antioxidants such as 2,4-di-*tert*-butylphenol, and 2,6-di-*tert*-*p*-benzoquinone are added to PEX pipes during the manufacturing process to prevent their oxidation by chlorinated drinking water.¹⁰ However, leaching of these antioxidants out of the plastic pipes during the first couple of years of their service makes them susceptible to oxidation by chlorine residues.^{7,8} Field investigations have demonstrated the formation of carbonyl ($>\text{C}=\text{O}$) and ether ($>\text{C}-\text{O}-\text{C}<$) functional groups on the surface of PEX pipes as a result of exposure to chlorinated water.^{9,11}

The mechanism by which polyethylene degrades has been depicted as initiating *via* a hydrogen abstraction process, followed by the formation of free radicals, then the generation of peroxy radicals, finally resulting in the creation of alcohols, acids, aldehydes, ketones, and unsaturated groups.^{12,13} Carbonyl groups on the plastic pipe surfaces are formed due to the chlorine free radicals attacking the pipe material, where hydrogen abstraction is followed by oxygen insertion.¹⁴⁻¹⁶ Plastic pipes exposed to aqueous free chlorine solution undergo surface oxidation, polymer chain scission, and finally, mechanical failure whereby cracks develop along the pipe wall.¹⁶ Carbonyl groups are the foremost indicators of polyethylene degradation and the formation of said group on the pipe surface occurs following exposure to chloramine and chlorine dioxide. HDPE and PEX pipes were found to age at a concentration of free chlorine of 2 mg L^{-1} concentration, which is typically present within drinking water.¹⁷ In addition to the durability issues raised by the oxidation of plastic pipes, the polar surface functional groups created on the plastic surface as the result of this oxidation may alter the physiochemical interactions of the pipe surface with the chemical and microbiological contaminants that are generally present within tap water, enhancing the risk of the accumulation of these contaminants on the pipe surface.³

Heavy metals can be released into plastic potable water plumbing systems from untreated water sources [*e.g.*, Fe, As],

as a result of certain treatment practices [*e.g.*, Mg, Mn], from water distribution systems [*e.g.*, Fe], and from building plumbing systems [*e.g.*, Cu, Pb].¹⁸⁻²⁰ Previous studies have shown that the release of metals from metallic pipes and brass fittings occurs through leaching.²¹ Metal-plastic hybrid potable water plumbing is commonly found within residential buildings, as existing metallic pipes are partially replaced with new plastic pipes (Fig. 1). In the case of the complete replacement of metallic pipes with plastic pipes, metallic fittings such as brass connections, valves, and copper elbows are still used.²² Moreover, many plastic potable water pipes are connected to metallic service lines [*e.g.*, lead, copper]. A recent study reported that metal deposition had occurred on downstream PEX pipes due to the corrosion of upstream copper pipes and brass fittings.¹⁸ The accumulation of Ca, Mn, and Zn onto downstream HDPE water mains has also been reported.²³

There is extensive literature regarding investigations on the effect that microplastic aging has on the heavy metal adsorption behavior of microplastics in the marine environment.²⁴ However, only a few studies have examined this process in potable water systems. Degraded microplastics have a greater heavy metal adsorption capacity than virgin microplastics as the degradation alters their physicochemical properties, such as the surface functional groups, specific surface area, and zeta potential.²⁵⁻²⁷ Heavy metal adsorption varies depending on the plastic type and the state of aging.²⁸⁻³³ Salehi *et al.* (2017) and Holmes *et al.* 2012 & 2014 reported increased adsorption of Cd, Co, Cr, Cu, Ni, and Pb on aged polyethylene compared to new plastic. The oxidized surface functional groups present in the plastic structure were found to be responsible for the greater metal uptake.^{11,32,33} Holmes *et al.* (2012) reported that the adsorption process achieved equilibrium on new and aged pellets within 25 h to 100 h of exposure.³³ Li *et al.* (2020) demonstrated that microplastics degraded by UV and chromic acid adsorbed a greater level of heavy metals than new microplastics.³⁴ Of the various heavy metals that are released by potable water plumbing materials, there is a significant human health concern associated with exposure to lead (Pb) through tap water. Depending on the source, water chemistry, and water flow conditions, lead can be released in dissolved and particulate forms into tap water.



Fig. 1 Connection of PVC potable water pipe to a copper pipe.

Particulate lead is defined as the portion of lead retained by a 0.45 μm filter. The major distinction between particulate and soluble lead is the impact of the water flow rate on their release behavior, in which an increased water flow rate is likely to enhance particulate lead release but reduce the dissolved lead concentration in water.^{35,36} A few recent studies have focused on the accumulation of particulate metals onto plastic piping materials. For instance, a study conducted by Cerrato *et al.* (2006) reported the deposition of manganese onto polyvinyl chloride (PVC) and iron pipe materials. A distinct thin brown layer containing particulate manganese (6% by weight) was found on PVC pipes, which was easily dislodged by flowing water, and contributed to the production of black water. However, the detachment of particulate manganese was found to be less in iron pipes due to their roughness compared to PVC pipes.³⁷ A study conducted by González *et al.* (2022) solely focused on the physicochemical properties of water that result in CaCO_3 scale formation on PVC pipes. However, the role of the pipe surface characteristics in the scale formation process has not been discussed.³⁸ A study conducted by Kettrane and Yahiaoui (2021) showed that CaCO_3 scale forms more in the aqueous phase than on the surface of HDPE pipes. However, no mechanistic discussion is provided on the role of plastic pipes in providing nucleation sites.³⁹ Although most of the prior studies focused on the release mechanisms of particulate lead, no attention has been paid to the transport of this particulate matter through the building's plumbing system and its subsequent deposition onto downstream plastic piping materials in distinction with dissolved lead species.

The physical confinement of heavy metals onto the plastic surface and the electrostatic interactions and chemical association between heavy metal species and plastic surface functional groups can be impacted by surface morphological and chemical changes caused by plastic degradation and environmental weathering.^{40–42} Previous studies have demonstrated that oxidized LDPE pellets and films have a higher surface area and hydrophilicity than new LDPE, resulting in greater Pb^{2+} , Cu^{2+} , Mn^{2+} , and Zn^{2+} uptake from water.^{3,42} Mao *et al.* (2020) studied the adsorption of Pb^{2+} , Cu^{2+} , Cd^{2+} , Ni^{2+} , and Zn^{2+} onto new and aged polystyrene (PS) and reported an increased adsorption capacity as a function of aging intensity. This could be attributed to changes in the physicochemical features of the PS, such as surface roughening and the emergence of oxygen-containing groups on the PS surface.²⁶ Evidence from the plastic pollution literature also showed that other plastics such as HDPE and PVC sorb heavy metals.^{33,43} However, information regarding the influence of plastic pipe surface aging on heavy metal deposition on said surface is lacking. Thus, this study aimed to investigate the influence of plastic pipe surface oxidation on Pb deposition behavior for PEX-A and HDPE pipes. The specific research objectives were to (1) examine the surface chemistry changes of plastic pipes due to aging in the presence of chlorine, (2) investigate the kinetics of Pb

deposition onto new and aged plastic pipes, and (3) identify the influence that the initial concentration of Pb has on its rate of deposition onto the plastic pipes.

Experimental

Materials

Cross-linked polyethylene-A (PEX-A) and high-density polyethylene (HDPE) pipes were purchased from local store (Memphis, USA). The internal diameters of the PEX-A and HDPE pipes were 1.7 and 2.1 cm, respectively. Lead (Pb) ICP-MS standard (1000 mg L⁻¹ in 3% nitric acid) was purchased from RICCA Chemical Company (Arlington, TX, USA). The 7.1% sodium hypochlorite (NaOCl) solution was obtained from a local store (Memphis, TN, USA). Nitric acids (68% purity) were purchased from Fisher Scientific (Hanover Park, IL, USA). All the experiments were conducted using Ultrapure Milli-QTM (18 M Ω cm) treated water unless described otherwise.

Pipe disinfection and accelerated aging experiments

The PEX-A and HDPE pipes were rinsed with tap water and disinfected with chlorinated water to clean the manufacturing residues prior to the experiments. For this purpose, the pipes were filled with an approximately 100 mg L⁻¹ total Cl_2 solution prepared using tap water and kept for 24 h at room temperature.⁴⁴ Then, the chlorinated waters were dumped, and the pipes were rinsed with tap water and ultrapure water. The accelerated aging process of the plastic pipes was conducted by filling the plastic pipe segments with a 5000 mg L⁻¹ total Cl_2 chlorine water solution at 70 °C, at pH 6.5 for up to 14 d. This solution was made by the addition of 1.4 mL of NaOCl solution (7.1%) to tap water. Its total chlorine concentration (the sum of the free and combined chlorine) was measured using a Hach Pocket Colorimeter IITM and total chlorine DPD reagents. The pH was adjusted to 6.5 by the addition of HNO_3 and HCl to the solution. The chlorinated water was stagnant in the filled pipes during this aging process, and the contact water was replaced every 3 d with newly prepared fresh chlorinated water.⁴⁵ To fill all the pipes with chlorinated water, both ends of the pipes were sealed with PTFE-wrapped rubber stoppers and placed in an electric oven to maintain the temperature at 70 °C. After 7 d, some of the pipe sections were collected for ATR-FTIR analysis, and the rest of the pipes were removed from the oven after 14 d. Then, the chlorinated water was dumped from the pipes and rinsed with tap water and ultrapure water prior to further experiments and analysis.

Surface chemistry characterization

(a) Attenuated total reflectance-Fourier transform infrared (ATR-FTIR) spectroscopy. The ATR-FTIR absorption spectra were acquired using a PerkinElmer Universal ATR-FTIR spectrophotometer in the range 4000 to 400 cm⁻¹ at an 8 cm⁻¹ spectral resolution. Polymer oxidation has been

frequently estimated using the intensity of carbonyl and vinyl bonds.^{46–48} In this study, the extent of the pipe surface aging was examined by determining the development of carbonyl and vinyl groups at wavenumber 1715 cm^{−1} and 909 cm^{−1}, respectively.^{48,49} Using eqn (1) and (2), carbonyl index (CI) and vinyl index (VI) values were determined, where A_{2870} , A_{1715} , and A_{909} represent the absorbance of methylene ($>\text{CH}_2$), carbonyl ($>\text{C}=\text{O}$), and vinyl ($>\text{CH}_2=\text{CH}_2<$) functional groups, respectively.^{47,48}

$$\text{Carbonyl index (CI)} = A_{1715}/A_{2870} \quad (1)$$

$$\text{Vinyl index (VI)} = A_{909}/A_{2870} \quad (2)$$

(b) X-ray photoelectron spectroscopy (XPS). X-ray photoelectron spectroscopy (XPS) measurements were accomplished using a Thermo Scientific K-Alpha XPS equipped with a monochromatic Al K α radiation source ($h\nu = 1486.6$ eV). The X-ray source operating power was 75 W at 12 kV, and the analysis area was 400 μm^2 for each sample. During the experiment, the analysis chamber base pressure was maintained at 8.0×10^{-10} mbar. The instrument was calibrated to maintain a binding energy of 284.6 eV for the C 1s adventitious (aliphatic) carbon line that appears on the non-sputtered samples. Photoelectrons were accumulated from a 90° take-off angle relative to the sample surface. The survey spectra were taken with a pass energy of 200 eV, and the high-resolution spectra were taken at 40 eV, with a 0.1 eV energy step size, using an average of 40 scans. The XPS data analysis was accomplished using the Thermo Avantage Software v5.995. Gaussian Lorentzian peaks were used for fitting all the core-level experimental data, and Shirley backgrounds were used as background corrections.^{3,50}

(c) Zeta potential measurement. Zeta potential measurements were carried out on new and aged HDPE pipes to determine how the surface charge of the plastic pipe fluctuates following pipe surface degradation. The measurements were conducted using an electrokinetic analyzer (SurPASS, 2010 model, Anton Paar USA, Ashland, VA, USA). To mount the sample for analysis, special adapters were created to fit the inside diameter of the pipes and link them with the outer diameter of the fluid nozzles on the analyzer. The pipe was then squeezed into a narrow channel by being clamped between two custom-made metal bars, about six inches (15 cm) long (Fig. S1†). A beaker containing a 500 mL solution of 1 mM KCl was fed to the instrument. Between 50 and 200 mL of the solution was pumped through the channel while the flow ramped up gradually to a pressure of 300 mbar. An electrical current was induced as a result of the interaction between the inner pipe surface and the electrolyte solution, which produced an electrical double layer.⁵¹ The zeta potential was calculated by the instrument software using the current that was observed during the flow rate ramp.

A titration was carried out automatically. The zeta potential was first measured at the original solution pH

(typically between 5.5 and 6). Then, small doses (~ 0.1 mL) of 0.1 N HCl were added to the solution until the pH dropped by at least 0.3 pH units. The zeta potential was assessed four times (twice in the forward flow direction and twice in the reverse flow direction). The pH was adjusted again, and the zeta potential was measured again. This continued until the pH of the solution reached almost 3. The solution was replaced with a fresh 500 mL of 0.1 mM KCl, and a similar titration was carried out using 0.1 N NaOH until the pH was close to 9. The titration and testing process took three to four hours in total. A titration curve of zeta potential against pH between 3 and 9 was produced using the combined data from the two experiments.

(d) Metal exposure experiments. The new and aged PEX-A and HDPE pipes were cut into 30 cm segments for Pb exposure experiments. Synthetic tap water was used; the constituents of synthetic tap water are given in Table S1.† For the kinetics experiments, 18 pipe segments were utilized to give three replicates for 6 time intervals (2, 6, 12, 24, 48, and 120 h). The segments were filled with 300 $\mu\text{g L}^{-1}$ Pb solution at pH = 7.8. To examine conditions that result in more serious health concerns, lead concentrations above the USEPA action level of 15 $\mu\text{g L}^{-1}$ were selected in this study. To study the influence of the initial Pb concentration on its rate of deposition onto the pipes, three replicate pipe segments were filled with Pb aqueous solution at five concentrations (50, 150, 500, 750, and 1000 $\mu\text{g L}^{-1}$) at pH = 7.8. The solution pH was adjusted using sodium hydroxide (NaOH) and hydrochloric acid (HCl). An Oakton® pH 450 portable pH meter was used to measure the pH of the solutions. To make sure we have a uniform distribution of lead species in the aqueous lead solutions, the solution was mixed thoroughly right before delivering the aliquot to the pipe segments. Pipe ends were sealed with PTFE-wrapped rubber stoppers and were placed horizontally on a benchtop at room temperature during the metal exposure experiments to avoid the potential deposition of lead precipitates on the PTFE caps. For kinetics experiments, three replicates were removed after each time interval, and the solution was collected for Pb quantification. PTFE caps were removed, and the solution was gently dumped into a plastic bottle, acidified with nitric acid for 24 h, and then a subsample was collected for metal quantifications.

The Pb uptake of the PTFE-wrapped stoppers after 5 d of kinetics experiments was analyzed as a control sample. The results showed that the PTFE wraps of the two stoppers used for each pipe section accumulated 0.5% of the total amount of Pb exposed to each pipe section after 5 d of metal exposure during the kinetics experiments. Due to its small value, we have neglected this in determining the metal uptake by the pipes. However, for the experiments conducted to study the impact of the initial Pb concentration, the samples were removed after 48 h, and

the solution was analyzed for the Pb quantifications. To quantify the remaining Pb in the solutions, concentrated nitric acid was added to make all the solutions 2% nitric acid solutions. The solutions were analyzed using a PerkinElmer Analyst 400 atomic absorption spectrometer attached to an HGA 900 graphite furnace to quantify the Pb concentrations. A Pb calibration curve was prepared using 0, 5, 10, 25, 50, 75, and 100 $\mu\text{g L}^{-1}$ of Pb solutions with the coefficient of determination (r^2) value 0.993, and a detection limit of 10 $\mu\text{g L}^{-1}$. The statistical analysis is described in the ESI† section (S1).

(e) Kinetics modeling. The kinetics of Pb deposition onto the new and aged plastic pipes were investigated through first-order (FO) (eqn (3)–(5)) and second-order (SO) kinetics models (eqn (6) and (7)),^{40,52} where t is time, q_t is the Pb surface loading at time t , q_e is the Pb surface loading at equilibrium, and k_1 and k_2 are the FO and SO rate constants, respectively. The half-life, $t_{1/2}$, is the amount of time needed for the pipe to deposit half of the equilibrium Pb surface loading.³⁹ The FO kinetics model best describes the physical adsorption process. It assumes that the rate of deposition of the solute onto the adsorbent is proportional to the difference between the saturation surface loading and the amount of adsorbed solute over time, as shown in eqn (3). But the SO kinetics model best describes the chemical associations between the adsorbents and adsorbate species during the adsorption process.⁵³ The SO model assumes that the rate-controlling step is the chemical association between the solute and adsorbate surface functional groups.²⁴ Chi-square (χ^2) was employed as a goodness of fit test by comparing the equilibrium adsorption data from the experiments and those calculated from the models (eqn (8)).⁵⁴ The parameters $q_{e,\text{exp}}$, and $q_{e,\text{m}}$ are the experimental and calculated model equilibrium adsorption data, respectively.

$$\frac{dq_t}{dt} = k_1(q_e - q_t) \quad (3)$$

$$q_t = q_e(1 - e^{-k_1 t}) \quad (4)$$

$$t_{1/2} = \frac{\ln 2}{k_1} \quad (5)$$

$$\frac{dq_t}{dt} = k_2(q_e - q_t)^2 \quad (6)$$

$$q_t = \frac{q_e k_2 t}{1 + q_e k_2 t} \quad (7)$$

$$\chi^2 = \sum_{i=1}^n \frac{(q_{e,\text{exp}} - q_{e,\text{m}})^2}{q_{e,\text{m}}} \quad (8)$$

Results and discussions

Plastic pipe surface chemistry variations due to aging

(a) ATR-FTIR spectroscopy. The ATR-FTIR spectroscopy analysis of new and aged plastic pipes revealed significant differences between the PEX-A and HDPE pipes due to the accelerated aging process. As shown in Fig. 2a, the characteristic ATR-FTIR bands of the new PEX-A pipes are the asymmetric band of the $>\text{C}-\text{H}$ stretching at 2915 cm^{-1} , the symmetric band of the $>\text{C}-\text{H}$ stretching at 2846 cm^{-1} , the $>\text{CH}_2$ symmetric bending vibrations at 1470 cm^{-1} and the $>\text{CH}_2$ asymmetric bending vibrations at 1465 cm^{-1} . Moreover, the $>\text{CH}_3$ bending vibrations appeared at 1370 cm^{-1} , and the $>\text{CH}_2$ rocking vibration was found at 730 cm^{-1} .^{55,56} For the PEX-A pipe that underwent 7 d of accelerated aging, new peaks appeared at 1715 cm^{-1} , 1260 cm^{-1} , and 909 cm^{-1} , which indicate the formation of carbonyl ($>\text{C}=\text{O}$), ether ($>\text{C}-\text{O}-\text{C}$), and vinyl ($>\text{C}=\text{C}$) groups, respectively, on the inner surface of the PEX-A pipes.⁵⁷ The presence of the $>\text{C}=\text{O}$ functional group is an important indicator of PEX-A pipe aging and the subsequent formation of aldehydes, ketones, or carboxylic acids on its surface. The presence of vinyl groups at the end of the polymeric chain leads to chain scission.⁵⁷ The carbonyl and vinyl indices of the new PEX-A pipe increased from 0.25 to 0.69 and from 0.27 to 0.82, respectively, after 7 d of aging. However, the extent of the PEX-A pipes aging remained almost unchanged even after undergoing an additional 7 d aging under similar conditions. This could be due to the limited strength of the chlorinated aqueous solution in affecting further degradation of the PEX pipe, as suggested by the literature.⁵⁸ Whelton *et al.* (2011) also reported that accelerated aging using 45 mg L^{-1} free chlorine at pH 6.5 for 141 d at 37 °C left no impact on the bulk or surface characteristics of the PEX-A pipe.⁸ The aging of PEX-A was confirmed by studies that show that degradation and even chain scissions occur due to the presence of oxidized functional groups and unsaturated carbon–carbon double bonds.^{11,48,59} Our previous study on exhumed one year-old PEX-A pipes used for hot and even cold water supply in a residential plumbing system in Indiana revealed that the white PEX-A pipe became yellowish and oxidized groups, such as $>\text{C}-\text{O}-\text{C}$ and $>\text{C}-\text{O}$, were found on the inner surface of the pipes, thus confirming that degradation had occurred.

The characteristic ATR-FTIR spectra of the new and aged HDPE pipes are shown in Fig. 2b. The main three methylene ($>\text{CH}_2$) group absorption peaks appeared as doublets at 2917 and 2849 cm^{-1} (asymmetric and symmetric stretching), 1472 and 1460 cm^{-1} (bending angular strain), and 730 and 718 cm^{-1} (rocking), respectively.^{60,61} New peaks appeared due to the HDPE pipe aging in the form of a broad hydroxyl ($>\text{O}-\text{H}$) peak at around 3370 cm^{-1} , a carbonyl ($>\text{C}=\text{O}$) peak at 1650 cm^{-1} , and a vinyl ($>\text{C}=\text{C}$) peak at 909 cm^{-1} .^{60,62} The carbonyl and vinyl indices were 0.54 and 0.64 for the new HDPE pipe, and were increased to 0.84 and 1.11, respectively, following 7 d of aging. By extending the degradation process up to a total

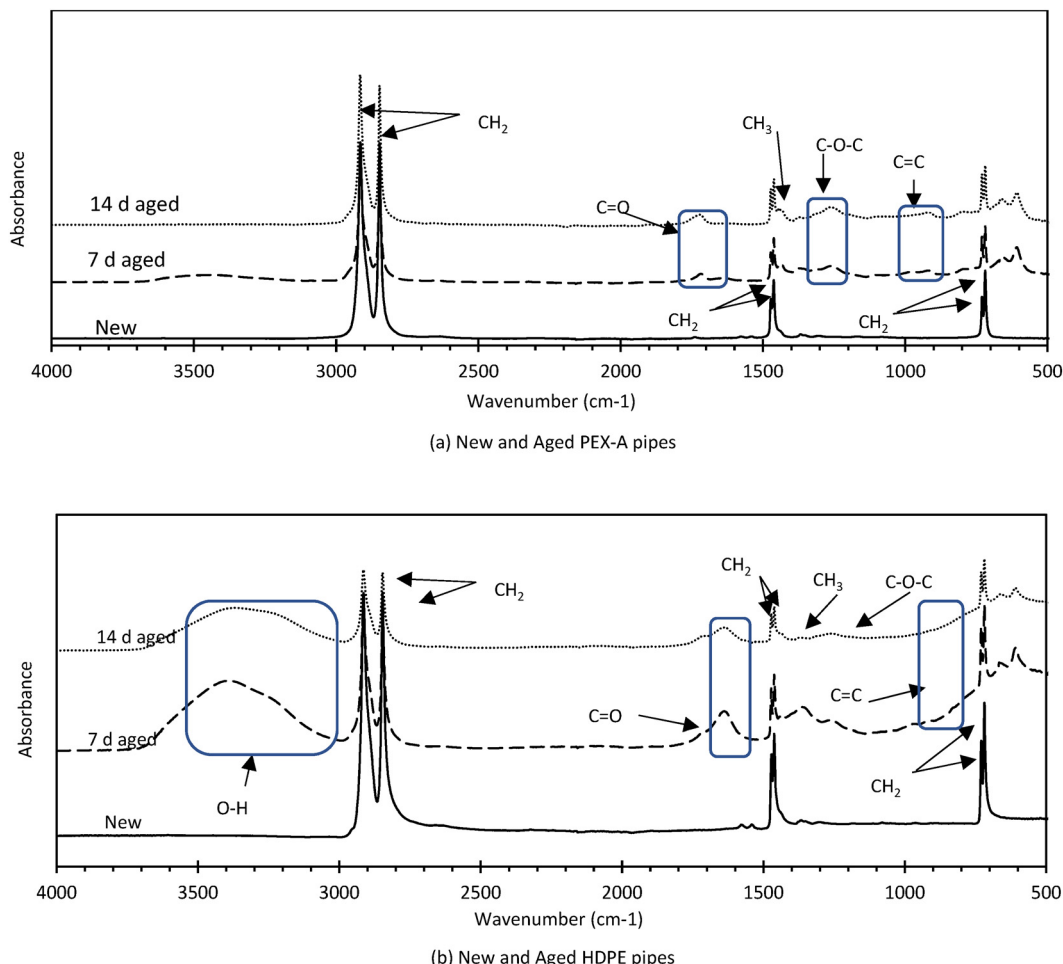


Fig. 2 ATR-FTIR spectra of new, 7 d, and 14 d aged (a) PEX-A and (b) HDPE plastic pipes.

of 14 d, unlike with the PEX-A pipes, the HDPE pipes showed enhanced degradation and the carbonyl and vinyl indices increased to 0.95 and 1.12, respectively. This difference in the aging behavior of the PEX-A and HDPE pipes at an increased duration of aging, in addition to their microstructural differences, might be related to the type and percentage of the antioxidants present within their structure. Our results agree with recently published studies that reported the appearance of carbonyl ($>\text{C}=\text{O}$) functional groups on an HDPE pipe surface due to accelerated degradation (45 mg L⁻¹ as Cl₂, 50 mg L⁻¹ alkalinity, pH 6.5, temperature 37 °C, and exposure 141 d).⁸

(b) X-ray photoelectron spectroscopy (XPS) analysis. An XPS analysis was conducted to have a better understanding of the extent of the oxidized surface functional groups that were formed on the pipes due to the accelerated aging experiments. Analyzing the XPS survey spectra of random samples taken from the new and aged PEX-A and HDPE pipes revealed a strong peak at 284.9–285.0 eV for the convoluted C 1s and a comparatively weaker peak at 534.1 eV for O 1s (Fig. S2†).^{18,63} In addition to carbon and oxygen, chlorine was also detected on the pipe surface due to its use in the accelerated aging experiments, despite

rinsing the pipes after the aging experiments with tap water and then with ultrapure water. The elemental atomic percentage (%) of C and O was resolved with 0.1% uncertainty by analyzing the high-resolution XPS spectra (Table 1). Fig. 3 shows the deconvolution of the C 1s high-resolution spectra into three or four subpeaks (e.g., $>\text{C}-\text{C}/>\text{C}-\text{H}$, $>\text{C}-\text{O}$, $>\text{O}-\text{C}-\text{O}</>\text{C}=\text{O}$, and $>\text{O}-\text{C}=\text{O}$).⁶⁴ The deconvoluted subpeaks are assigned as $>\text{C}-\text{C}/>\text{C}-\text{H}$, $>\text{C}-\text{O}$, $>\text{O}-\text{C}-\text{O}</>\text{C}=\text{O}$, and $>\text{O}-\text{C}=\text{O}$ with corresponding

Table 1 Elemental atomic concentration (%) of new and aged PEX-A and HDPE pipe samples at a 0.1% level of uncertainty

Parameters	C 1s						
	C-C	C-O	C=O	O-C=O	O 1s	Cl 2p	C _{ox} /C _{unox}
PEX-A New	80.4				15.0	4.6	
	77.2	17.6	—	5.2			0.3
14 d aged	77.2				9.4	13.3	
	71.1	27.0	—	2.0			0.4
HDPE New	90.7				8.1	1.2	
	90.8	7.8	1.4	—			0.1
14 d aged	73.6				9.3	17.1	
	67.7	23.7	5.5	3.0			0.5

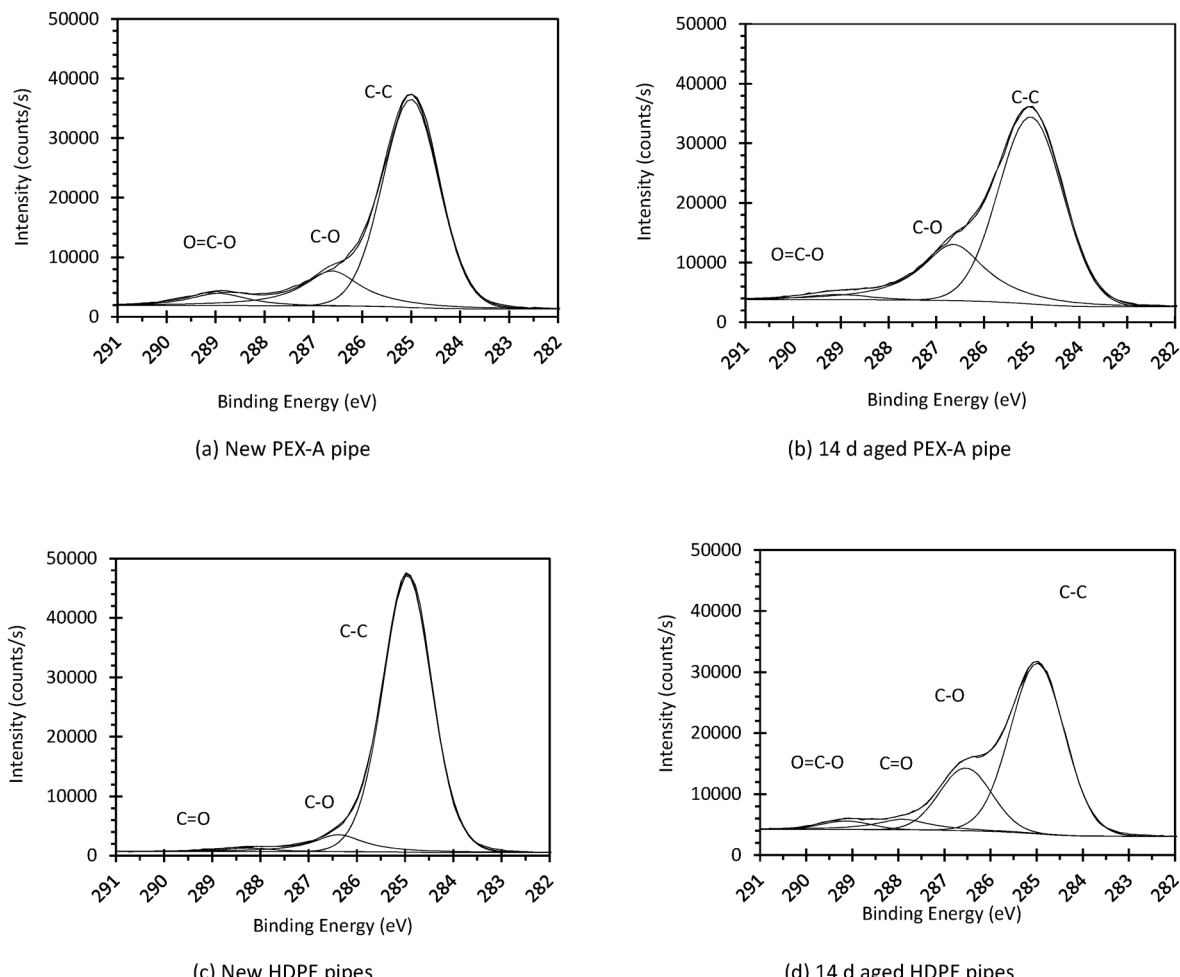


Fig. 3 High-resolution deconvoluted C 1s spectra of (a) new PEX-A, (b) 14 d aged PEX-A, (c) new HDPE, and (d) 14 d aged HDPE pipes.

binding energies at 284.95–285.02, 286.38–286.64, 287.91–288.25, and 288.94–289.50 eV, respectively.^{63,64} It is possible that the O 1s peaks for the new PEX-A and HDPE samples are the result of their inherent surface oxidation. As shown in Table 1, after 14 d of aging the extent of the $>\text{C}-\text{C}<$ bonds in the new PEX-A and HDPE pipes reduced from 80.4% and 90.7% to 71.1% and 67.7%, respectively, due to the interaction of $>\text{C}-\text{C}<$ with the chlorine residuals $[\text{OCl}^-]$, HOCl present in the aqueous system. The extent of the $>\text{C}-\text{C}<$ bonds in the new PEX-A and HDPE pipes reduced from 80.4% and 90.7% to 71.1% and 67.7%, respectively, after 14 d of aging.

On the other hand, the percentage of $>\text{C}-\text{O}<$ groups increased from 17.6% to 27% after the PEX-A pipes were aged for 14 d. Moreover, the percentage of $>\text{C}-\text{O}<$ and $>\text{C}=\text{O}<$ groups increased from 7.8% and 1.4% in the new HDPE pipes to 24% and 5.5% in the 14 d aged HDPE pipes. The degree of surface oxidation was calculated using the ratio of oxidized carbon to unoxidized carbon ($\text{C}_{\text{ox}}/\text{unox}$) and is shown in Table 1.⁶⁴ A greater degree of surface oxidation was found for HDPE pipes (0.5) compared to the PEX-A pipes (0.4) after undergoing 14 d of accelerated aging.

Variations in surface charge due to aging

Zeta potential measurements were conducted on representative samples from new and aged HDPE pipes to better understand how surface oxidation of this plastic pipe influences its electrostatic interactions with

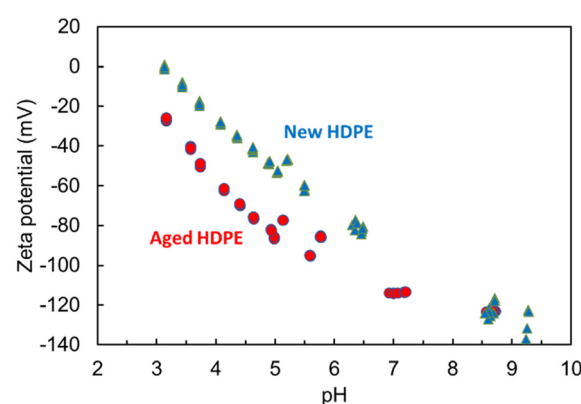


Fig. 4 Zeta potential of new and aged HDPE pipes as a function of pH.

the Pb species that are present in water. As shown in Fig. 4, the zeta potential for the new HDPE pipe varied between 0 and -137 mV, whereas it varied from -27 to -121 mV for the aged HDPE pipe. As the pH increased, the surface charge became more negative, as is typical for virtually all surfaces, due to lower H^+ and higher OH^- concentrations. The presence of oxidized carbon functional groups, such as carbonyl ($>C=O$), ether ($>C-O-C<$), and carboxyl ($>O-C=O<$) groups, on the aged HDPE surface increase the negative charge. This finding agrees with the results reported by Liu (2021), who also found a more negative surface charge for UV/ O_3 -treated poly(methyl methacrylate). The presence of oxygen-containing surface functional groups, specifically the carboxyl ($>COOH$) groups, was presented as the major contributor to the more negative surface charge.⁶⁵ Moreover, the study conducted by Asadinezhad *et al.* (2012) also demonstrated a more negative surface charge for plasma-treated PVC compared to new PVC samples due to the presence of a greater level of oxidized carbon surface functional groups [e.g., $>C=O$, $>COOH$, $>C-O-C<$].⁶⁶ A more negative surface charge may promote the electrostatic attraction of neutral and positively charged Pb species to the plastic pipe surface and consequently increases the surface deposition of Pb species.

Kinetics of lead deposition onto new and aged plastic pipes

The Pb deposition experiments were conducted using synthetic tap water at $pH = 7.8$ and an initial Pb concentration of $[Pb]_t = 300 \mu\text{g L}^{-1}$. Solving the relevant complexation and solubility reactions revealed that under these conditions majority of Pb is present as precipitate and only small percentage of Pb is dissolved. This indicates that for the kinetic experiments, in addition to the adsorption of dissolved Pb species onto the plastic pipe surface, precipitation also occurred. Thus, we refer to the Pb uptake by the plastic pipe surface as Pb deposition that involves adsorption and precipitation. As presented in our recent research, the metal species initially adsorbed onto the plastic surface could act as nucleation sites for the growth of metal crystals. Prior studies have shown that metals can associate with low-energy polymer surfaces, such as an attractive local arrangement of polymeric chains, surface impurities, and polymer terminal groups.^{67,68} For instance, the nucleation of $CaCO_3$ crystals was facilitated through the complexation of Ca^{2+} by the carboxylic acid groups that existed on the surface of grafted HDPE.⁶⁹

The kinetics of Pb deposition onto the plastic pipe surfaces was examined to better explain how aging and surface oxidation of the plastic pipe surface alters the physiochemical interactions of the surface with the Pb in the

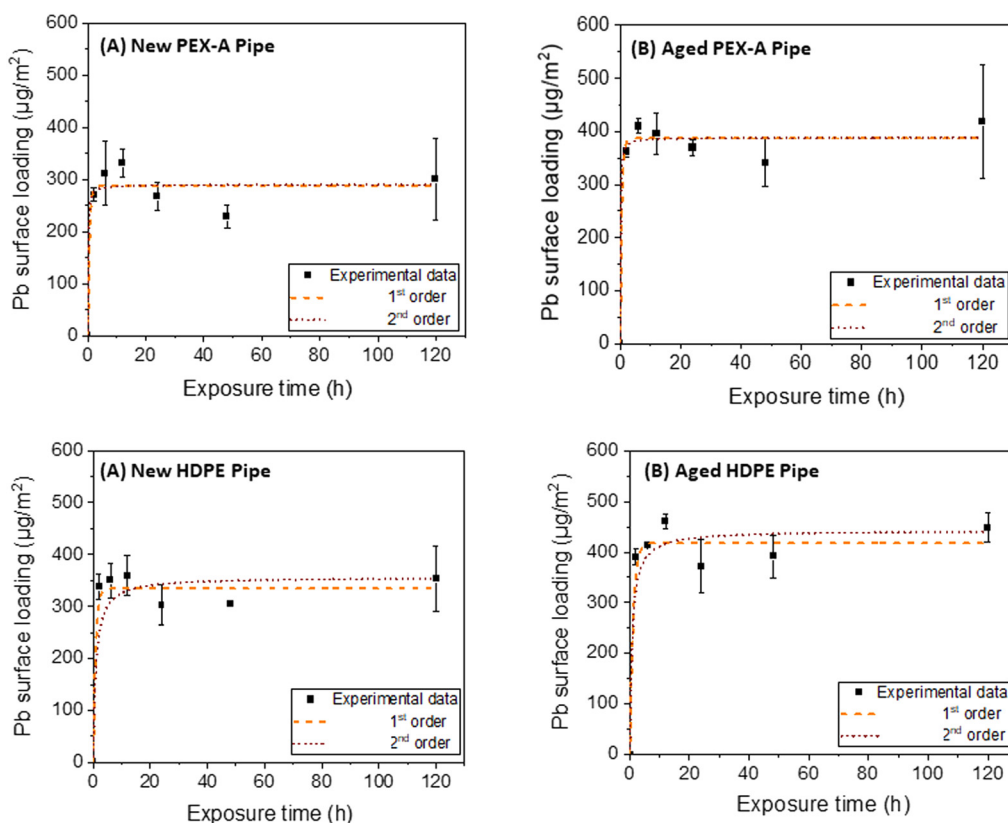


Fig. 5 First order (FO) and second order (SO) kinetics models for the accumulation of lead (Pb) onto (a) new PEX-A, (b) aged PEX-A, (c) new HDPE, and (d) aged HDPE pipes.

water. The Pb equilibrium surface loading showed that a significantly greater level (p value < 0.05) of Pb was deposited on the aged PEX-A pipes ($387 \mu\text{g m}^{-2}$) compared to the new PEX-A pipes ($288 \mu\text{g m}^{-2}$). Meanwhile, a significantly greater level (p value < 0.05) of Pb was deposited on the aged HDPE pipes ($418 \mu\text{g m}^{-2}$) than on the new HDPE pipes ($335 \mu\text{g m}^{-2}$) (Fig. 5). During the first two hours of exposure, 94.8% of its equilibrium Pb surface loading was deposited on the aged PEX-A pipe, whereas after 2 hours of exposure 94% of its equilibrium Pb surface loading was deposited on the new PEX-A pipe. During the first two hours of Pb exposure, the aged HDPE pipes showed a similar trend to the new and aged PEX-A pipes, where the aged HDPE pipes accumulated 92.8% of its equilibrium Pb surface loading whilst the new HDPE pipe accumulated 100% of the equilibrium amount. The equilibrium Pb surface loading on the aged PEX-A pipe was 32% of the total Pb $[\text{Pb}]_t$ in the synthetic tap water, whereas the equilibrium Pb surface loading on the new PEX-A pipe was only 22.1%. Similar to the aged PEX-A pipes, the equilibrium surface loading of the aged HDPE pipes represented 32% of the total Pb $[\text{Pb}]_t$ in the synthetic tap water, whilst the new HDPE pipes accumulated only 24.0%. In addition, a comparison of the Pb deposition between the different pipe types showed that the surface loading of Pb onto the new HDPE pipe ($335 \mu\text{g m}^{-2}$) was significantly greater (p -value < 0.05) than on the new PEX-A pipe ($288 \mu\text{g m}^{-2}$). Similarly, a significantly greater (p -value < 0.05) amount of Pb was deposited on the aged HDPE pipes ($418 \mu\text{g m}^{-2}$) than on the aged PEX-A pipes ($387 \mu\text{g m}^{-2}$).

First-order (FO) and second-order (SO) kinetic models were used to describe the mechanisms by which Pb is deposited onto the plastic pipes. The FO model reveals a more physical process involving diffusion of adsorbate from the aqueous solution to the adsorbent surface.⁷⁰ However, the SO model considers the chemical association to be the rate-controlling step.^{54,71} The non-linear FO and SO models were compared using a non-linear chi-square (χ^2) test to ascertain which model better suited the kinetics of Pb deposition onto the plastic pipes (Table 2). The experimental data obtained from the deposition of Pb onto the new and aged PEX-A and HDPE pipes were fitted to the non-linear FO and SO models. While the model fits are visually quite similar for the PEX-A data (Fig. 5a and b), there is a slight difference in visual fit for the HDPE data (Fig. 5c and d). The χ^2 values of the FO models were found to be slightly smaller than for the SO models for all the studied pipes, lending

some support to the idea that physical adsorption is a more dominant mechanism than chemisorption. In this study, surface diffusion plays a greater role in Pb deposition onto the pipes than rate-controlled chemical association processes. This is shown by the fact that the calculated χ^2 values for the aged pipes using the first order and second order models were so similar to each other. The half-life ($t_{1/2}$) calculation revealed that the half-life durations for degraded (0.4 h) and new (0.4 h) PEX-A were similar. However, the half-life for aged HDPE (0.8 h) pipes was slightly greater than for new HDPE (0.6 h) pipes.

Influence of initial Pb concentration on its deposition rate onto new and aged plastic pipes

The influence of the initial Pb concentration on the rate of its deposition onto new and aged plastic pipes was investigated. At equilibrium, the Pb surface loading with respect to the residual Pb concentration remaining in the solution was plotted and the slopes were determined as the rate of Pb deposition. A linear regression revealed that as the initial Pb concentration increased from $50 \mu\text{g L}^{-1}$ to $1000 \mu\text{g L}^{-1}$, the Pb surface loadings on the aged and new PEX-A pipes increased linearly with a very good coefficient of determination (r^2) (Fig. 6a). The r^2 values for the aged PEX-A and new PEX-A pipes were 0.96 and 0.97, respectively. The maximum Pb surface loading onto the aged PEX-A pipes was found to be $2304 \mu\text{g m}^{-2}$ greater than the Pb surface loadings onto the new PEX-A pipes ($1859 \mu\text{g m}^{-2}$), although this difference was not significant (p -value > 0.05). However, the rate of Pb deposition onto the aged PEX-A pipes was found to be greater than on the new PEX-A pipes and the difference was statistically significant (p -value < 0.05). This maximum Pb surface loading obtained by our bench-scale experiments is within the range of Pb loadings reported from experiments conducted in the field. For instance, a study conducted by Huang *et al.* (2019) showed that a six-month-old exhumed PEX-A pipe from a U.S. residential house contained $100\text{--}135 200 \mu\text{g m}^{-2}$ Pb surface loading. This metal deposition on the PEX-A pipes can be attributed to the possible formation of metal oxides and oxyhydrides at elevated temperatures and a slightly basic system within the potable water plumbing.^{72,73}

The Pb surface loading onto the new and aged HDPE pipes increased linearly as the initial Pb concentration increased from $50 \mu\text{g L}^{-1}$ to $1000 \mu\text{g L}^{-1}$ (Fig. 6b). The r^2

Table 2 Kinetics model parameters and non-linear chi-square (χ^2) values for Pb accumulation on new and aged plastic pipes

Samples		1st order				2nd order			$q_e (\mu\text{g m}^{-2})$	
Models	Parameters	$q_{e,\text{model}} (\mu\text{g m}^{-2})$	$K_1 (\text{h}^{-1})$	$t_{1/2} (\text{h})$	χ^2	$q_{e,\text{model}} (\mu\text{g m}^{-2})$	$K_2 (\text{m}^2 \mu\text{g}^{-1} \text{h}^{-1})$	$t_{1/2} (\text{h})$	experimental	χ^2
PEX-A	New	288	1.89	0.4	1.88	290	0.030	0.03	265	2.20
	14 d aged	387	1.91	0.4	0.13	389	0.030	0.03	380	0.20
HDPE	New	335	1.20	0.6	0.12	356	0.003	0.24	329	2.12
	14 d aged	418	0.91	0.8	0.01	443	0.003	0.24	420	1.17

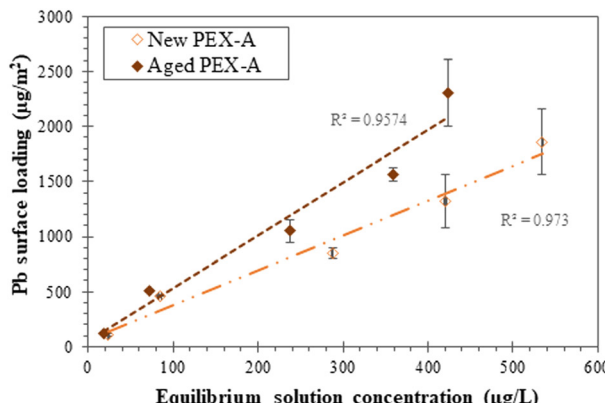
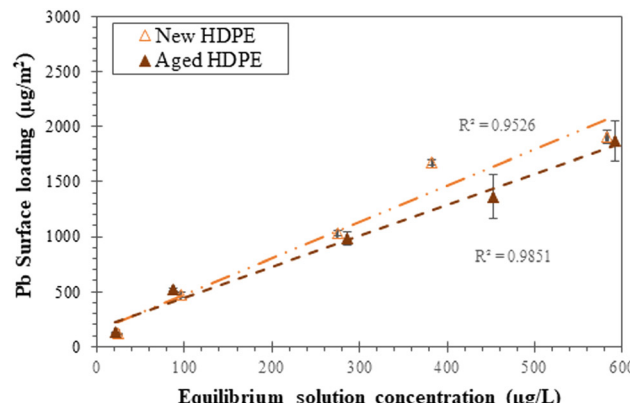


Fig. 6 Equilibrium Pb surface loading with respect to the residual Pb in the bulk solution for new and aged (a) PEX-A and (b) HDPE pipes.



values for the aged and new HDPE pipes were $r^2 = 0.99$ and $r^2 = 0.95$, respectively. Unlike the PEX-A pipes, the maximum Pb surface loading onto the aged HDPE pipes was found to be $1868 \mu\text{g m}^{-2}$, less than the maximum Pb surface loading onto the new HDPE pipes ($1909 \mu\text{g m}^{-2}$), although the difference was not statistically significant (p -value > 0.05). Similarly, the rate of Pb deposition onto the aged HDPE pipes was lower than onto the new HDPE pipes, and the difference was not statistically significant (p -value > 0.05). At lower initial concentrations of Pb^{2+} , the majority of the Pb species are present as dissolved species (Pb^{2+} , PbOH^+). Thus, surface adsorption is the process that controls the deposition of the Pb species onto the plastic pipe surface. However, as the initial Pb^{2+} concentration increases and exceeds the solubility constant of $\text{Pb}(\text{OH})_2$ (s) [$K_s^* = 10^{8.15}$] a precipitate is formed in the solution and on the inner surface of the plastic pipes. It is expected that an increasing level of lead precipitates will form in the aqueous system by raising the initial lead concentration. Thus, the process of lead uptake by water pipes was defined as a deposition process that involves both adsorption and precipitation processes. This is relevant to the real potable water plumbing conditions where the pipes are exposed to particulate lead in addition to dissolved lead in tap water. The excessive long-term release of lead particulate into tap water may occur by galvanic corrosion or disturbance of the pipe scale caused by partial replacement of lead service lines.⁷⁴ Although, in many field investigations, elevated lead levels have been associated with particulate lead, the critical role of particulate lead as a nucleation site for the growth of lead precipitate on the pipes' inner walls should not be ignored (Fig. 7). As reported in our previous research, metal species initially adsorbed onto plastic can act as nucleation sites for the growth of metal crystals and for precipitate to accumulate on the plastic surface (Fig. 7).¹⁰ Thus, at a lower range of Pb concentrations, the pipe age, and thus surface oxidation, influences the adsorption of Pb species. However, by increasing the initial Pb concentrations, we increased the layers of insoluble Pb species that precipitate onto the pipe surface, therefore we did not find a significant difference in

the maximum Pb surface loadings for the new and aged PEX-A and HDPE pipes.

Limitations and practical implications

This study was associated with some limitations in terms of conducting the accelerated aging process and running the metal exposure experiments only under stagnant conditions. Due to the logistic considerations required to complete the aging process within a short time period, the elevated dosage of free chlorine residues at high temperatures was utilized for the creation of oxidized surface functional groups on the pipe surfaces.^{9,45,75} However, under real operational conditions, the plastic potable water pipes are exposed to a lower concentration of free chlorine ($<2.0 \text{ mg L}^{-1}$) at lower temperatures for years. Moreover, although in this study the Pb exposure experiments were conducted only under stagnant conditions, the plastic pipes used for building plumbing experience both stagnant and flow conditions that vary based on the water use behavior of the building residents. Shorter contact time between the plastic pipe surface sites and metal species present in the water under water flow conditions and a greater mass transfer gradient adjacent to the pipe surface may alter the rate of Pb deposition onto the new and aged plastic pipes.

Moreover, this study showed a rapid deposition of the Pb species onto both new and aged plastic pipes. At least 92.8% of the equilibrium Pb surface loading on pipes was obtained within the first 2 h of the metal exposure period. However, no metal analysis was conducted during this initial exposure period to capture the early-stage kinetic variations for different pipes. Additionally, the kinetics experiments conducted in this study revealed a rapid uptake of lead by both new and aged plastic pipes. No dramatic increase in the lead surface loadings was found for the target new and aged pipes by increasing the exposure duration from 2 h to 5 d. The mass percentage of lead accumulated on the new and aged pipes did not exceed 24% and 32% of the total available lead in the aqueous system, respectively. This finding indicates the limitation of this study as, in real-life conditions, potable water plumbing may be subjected to

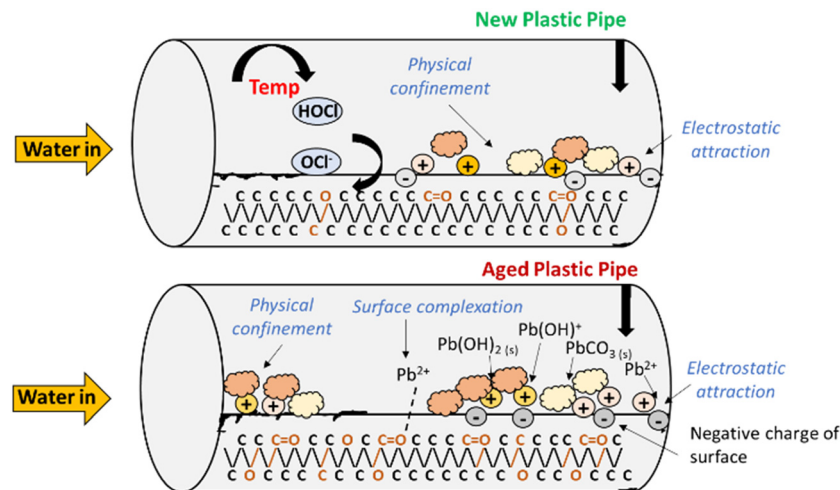


Fig. 7 Schematic drawing demonstrating the mechanisms leading to Pb deposition onto new and aged plastic water pipes.

chronic exposure to lead in tap water for significantly longer durations for those cases with lead service lines or sections of galvanized iron pipes. For instance, it took nearly a year of investigation for several instances in Washington DC (2003) to identify tap water as the source of children's elevated blood lead levels.⁷⁶ Thus, future investigation is needed to examine the kinetics of lead uptake by new and aged plastic plumbing materials in long-term exposure experiments. To achieve more representative results of real-building potable water plumbing conditions, future studies should consider the interconnected effects of water flow conditions and disinfectant residue decay while conducting long-term lead exposure experiments. Although this study does not distinguish between the interaction of dissolved lead species and particulate lead with the surface of plastic pipes, future research is needed to differentiate the adsorption of dissolved lead species from the surface accumulation of particulate lead. By investigating the interplay between dissolved and particulate lead, researchers can gain a more comprehensive understanding of the mechanisms of lead contamination in plumbing systems and develop strategies to mitigate the risks associated with both forms of lead.

Despite these limitations, this study provides valuable insight into the critical role that the surface aging/oxidation of plastic pipes plays on their association with Pb and, consequently, the Pb transport behavior. Antioxidants are added to plastic pipes during the manufacturing process to prevent their oxidation due to exposure to the disinfectant residuals in tap water. However, the gradual leaching of antioxidants out of the pipe structure over time makes plastic pipes more susceptible to aging, specifically those pipes carrying hot water. The creation of oxidized surface functional groups on the plastic surface and slight changes in the surface charge impact the physicochemical interactions of the pipe's inner walls with organic, inorganic, and microbiological contaminants present within tap water. Although this study only focused on Pb due to its significant acute and chronic toxic effects, future research is needed to

examine how plastic pipe surface aging impacts biofilm accumulation and organic contaminant adsorption onto the pipe surface. These biofilms can interact with heavy metals present in tap water through various potential mechanisms, including metal-mediated alterations in microbial communities, metal-mediated changes in biofilm gene expression, microbial-mediated biosorption, and microbial-mediated metal transformations.⁷⁷ Future, systematic investigation is needed to relate the plastic pipe surface chemistry variations to the biofilm growth and heavy metals accumulation in buildings' potable water plumbing systems. Moreover, this study only focused on the deposition of Pb species onto the pipes; future research is needed to identify the physicochemical drivers of Pb mobilization within the plastic potable water system.

Conclusions

In this study, the role that plastic potable water pipe surface aging plays in the mechanism of Pb deposition onto the inner surface of the pipes was examined under stagnant conditions. Accelerated aging using high concentration chlorine residues at an elevated temperature significantly altered the surface chemistry of the pipes by creating oxidized carbon functional groups [*e.g.*, $>\text{C}=\text{O}$, $>\text{C}-\text{O}-\text{C}<$]. The surface aging and formation of oxidized carbon functional groups made the plastic surface more negatively charged compared to new pipes. The kinetics experiments revealed a significantly greater level of Pb deposition onto the aged PEX-A and HDPE pipes compared to new pipes at equilibrium. A greater number of electrostatic interactions and potential surface complexations could have promoted Pb deposition onto the aged pipes compared to the new pipes. Increasing the initial Pb concentration resulted in increased Pb surface deposition onto the new and aged PEX-A and HDPE pipes. A greater rate of Pb deposition was found for aged PEX-A pipes compared to new PEX-A pipes. A kinetic study revealed rapid Pb deposition onto the new and aged

plastic pipes. The results of this study could serve as a foundation for future studies on the fate of heavy metals in water infrastructure.

Author contributions

Md Hadiuzzaman: investigation, analysis, visualization; David Ladner: methodology, editorial, analysis; Maryam Salehi: conceptualization, methodology, editorial, project administration, funding.

Conflicts of interest

The authors certify that they have NO affiliations with or involvement in any organization or entity with any financial interest or non-financial interest in the subject matter or materials discussed in this manuscript.

Acknowledgements

Funding for this work was provided by National Science Foundation grant CEBT-2029764. The authors thank Colton Kirby and Marvin Dassael Lopez for their assistance with the pipe loop experiments. The authors also thank Dr. Felio Perez for assistance with conducting the XPS analysis and Lingyun Peng for assistance with the surface charge analysis.

References

- 1 A. J. Whelton and T. Nguyen, Contaminant Migration from Polymeric Pipes Used in Buried Potable Water Distribution Systems: A Review, *Crit. Rev. Environ. Sci. Technol.*, 2013, **43**(7), 679–751.
- 2 T. Walsh, The Plastic Piping Industry in North America, in *Applied Plastics Engineering Handbook: Processing, Materials, and Applications*, ed. M. Kutz, William Andrew, Norwich, NY, 2nd edn, 2017, vol. 32, pp. 697–716.
- 3 M. Salehi, C. T. Jafvert, J. A. Howarter and A. J. Whelton, Investigation of the factors that influence lead accumulation onto polyethylene: Implication for potable water plumbing pipes, *J. Hazard. Mater.*, 2018, **347**, 242–251.
- 4 J. Lee, E. Kleczyk, D. J. Bosch, A. M. Dietrich, V. K. Lohani and G. V. Loganathan, Homeowners' decision-making in a premise plumbing failure-prone area, *J. - Am. Water Works Assoc.*, 2013, **105**(5), E236–E241.
- 5 X. Huang, S. Andry, J. Yaputri, D. Kelly, D. A. Ladner and A. J. Whelton, Crude oil contamination of plastic and copper drinking water pipes, *J. Hazard. Mater.*, 2017, **339**, 385–394.
- 6 Y. Zhang and M. Edwards, Anticipating effects of water quality changes on iron corrosion and red water, *J. Water Supply: Res. Technol.-AQUA*, 2007, **56**(1), 55–68.
- 7 A. J. Whelton, A. M. Dietrich, G. A. Burlingame, M. Schechs and S. E. Duncan, Minerals in drinking water: impacts on taste and importance to consumer health, *Water Sci. Technol.*, 2007, **55**(5), 283–291.
- 8 A. J. Whelton, M. Asce, A. M. Dietrich, A. Asce and D. L. Gallagher, Impact of Chlorinated Water Exposure on Contaminant Transport and Surface and Bulk Properties of High-Density Polyethylene and Cross-Linked Polyethylene Potable Water Pipes, *J. Environ. Eng.*, 2011, **137**(7), 559–568.
- 9 J. C. Montes, D. Cadoux, J. Creus, S. Touzain, E. Gaudichet-Maurin and O. Correc, Ageing of polyethylene at raised temperature in contact with chlorinated sanitary hot water, Part i - Chemical aspects, *Polym. Degrad. Stab.*, 2012, **97**(2), 149–157.
- 10 A. Pelto-Huikko, M. Ahonen, M. Ruismäki, T. Kaunisto and M. Latva, Migration of Volatile Organic Compounds(VOCs) from PEX-a Pipes into the Drinking Water during the First Five Years of Use, *Materials*, 2021, **14**(4), 1–11.
- 11 M. Salehi, X. Li and A. J. Whelton, Metal accumulation in representative plastic drinking water plumbing systems, *J. - Am. Water Works Assoc.*, 2017, **109**(11), E479–E493.
- 12 A. T. Halle, L. Ladirat, M. Martignac, A. F. Mingotaud, O. Boyron and E. Perez, To what extent are microplastics from the open ocean weathered?, *Environ. Pollut.*, 2017, **227**, 167–174.
- 13 M. Gardette, A. Perthue, J. L. Gardette, T. Janecska, E. Földes, B. Pukánszky and S. Therias, Photo- and thermal-oxidation of polyethylene: Comparison of mechanisms and influence of unsaturation content, *Polym. Degrad. Stab.*, 2013, **98**(11), 2383–2390.
- 14 J. Lacoste, D. J. Carlsson, S. Falicki and D. M. Wiles, Polyethylene hydroperoxide decomposition products, *Polym. Degrad. Stab.*, 1991, **34**(1–3), 309–323.
- 15 J. Hassinen, M. Lundbäck, M. Ifwarson and U. W. Gedde, Deterioration of polyethylene pipes exposed to chlorinated water, *Polym. Degrad. Stab.*, 2004, **84**(2), 261–267.
- 16 X. Colin, L. Audouin, J. Verdu, M. Rozental-Evesque, B. Rabaud, F. Martin and F. Bourgine, Aging of polyethylene pipes transporting drinking water disinfected by chlorine dioxidem, Part II-lifetime prediction, *Polym. Eng. Sci.*, 2009, **49**(8), 1642–1652.
- 17 T. H. Heim and A. M. Dietrich, Sensory aspects and water quality impacts of chlorinated and chloraminated drinking water in contact with HDPE and cPVC pipe, *Water Res.*, 2007, **41**(4), 757–764.
- 18 X. Huang, K. J. Pieper, H. K. Cooper, S. Diaz-Amaya, D. Y. Zemlyanov and A. J. Whelton, Corrosion of upstream metal plumbing components impact downstream PEX pipe surface deposits and degradation, *Chemosphere*, 2019, **236**, 124329.
- 19 S. Ghoochani, M. Salehi, D. DeSimone, M. S. Esfandarani and L. Bhattacharjee, Studying the impacts of non-routine extended schools' closure on heavy metal release into tap water, *Environ. Sci.: Water Res. Technol.*, 2022, **8**(6), 1223–1235.
- 20 M. Salehi, D. Desimone, K. Aghilinasrollahabadi and T. Ahamed, A case study on tap water quality in large buildings recommissioned after extended closure due to the COVID-19 pandemic, *Environ. Sci.: Water Res. Technol.*, 2021, **7**(11), 1996–2009.
- 21 K. J. Pieper, L. A. Krometis and M. Edwards, Quantifying lead-leaching potential from plumbing

exposed to aggressive waters, *J. Am. Water Works Assoc.*, 2016, **108**(9), E458–E466.

22 D. Brennecke, B. Duarte, F. Paiva, I. Caçador and J. Canning-Clode, Microplastics as vector for heavy metal contamination from the marine environment, *Estuarine, Coastal Shelf Sci.*, 2016, **178**, 189–195.

23 D. A. Lytle, T. J. Sorg, M. Christy and W. Lili, Particulate arsenic release in a drinking water distribution system, *J. Am. Water Works Assoc.*, 2010, **102**(3), 87–98.

24 A. Herath and M. Salehi, Studying the combined influence of microplastics' intrinsic and extrinsic characteristics on their weathering behavior and heavy metal transport in storm runoff, *Environ. Pollut.*, 2022, **308**, 119628.

25 P. Liu, L. Qian, H. Wang, X. Zhan, K. Lu, C. Gu and S. Gao, New Insights into the Aging Behavior of Microplastics Accelerated by Advanced Oxidation Processes, *Environ. Sci. Technol.*, 2019, **53**(7), 3579–3588.

26 R. Mao, M. Lang, M. Yu, R. Wu, X. Yang and X. Guo, Aging mechanism of microplastics with UV irradiation and its effects on the adsorption of heavy metals, *J. Hazard. Mater.*, 2020, **393**, 122515.

27 X. Gao, I. Hassan, Y. Peng, S. Huo and L. Ling, Behaviors and influencing factors of the heavy metals adsorption onto microplastics: A review, *J. Cleaner Prod.*, 2021, **319**, 128777.

28 E. Nakashima, A. Isobe, S. Kako, T. Itai and S. Takahashi, Quantification of toxic metals derived from macroplastic litter on Ookushi Beach, Japan, *Environ. Sci. Technol.*, 2012, **46**(18), 10099–10105.

29 J. Wang, J. Peng, Z. Tan, Y. Gao, Z. Zhan, Q. Chen and L. Cai, Microplastics in the surface sediments from the Beijiang River littoral zone: Composition, abundance, surface textures and interaction with heavy metals, *Chemosphere*, 2017, **171**, 248–258.

30 A. Turner and L. A. Holmes, Adsorption of trace metals by microplastic pellets in fresh water, *Environ. Chem.*, 2015, **12**(5), 600–610.

31 C. M. Rochman, B. T. Hentschel and S. J. Teh, Long-term sorption of metals is similar among plastic types: Implications for plastic debris in aquatic environments, *PLoS One*, 2014, **9**(1), e85433.

32 L. A. Holmes, A. Turner and R. C. Thompson, Interactions between trace metals and plastic production pellets under estuarine conditions, *Mar. Chem.*, 2014, **167**, 25–32.

33 L. A. Holmes, A. Turner and R. C. Thompson, Adsorption of trace metals to plastic resin pellets in the marine environment, *Environ. Pollut.*, 2012, **160**(1), 42–48.

34 Z. Li, X. Hu, L. Qin and D. Yin, Evaluating the effect of different modified microplastics on the availability of polycyclic aromatic hydrocarbons, *Water Res.*, 2020, **170**, 115290.

35 C. Cartier, R. B. Arnold, S. Triantafyllidou, M. Prévost and M. Edwards, Effect of flow rate and lead/copper pipe sequence on lead release from service lines, *Water Res.*, 2012, **46**(13), 4142–4152.

36 E. Deshommes, L. Laroche, S. Nour, C. Cartier and M. Prévost, Source and occurrence of particulate lead in tap water, *Water Res.*, 2010, **44**(12), 3734–3744.

37 J. M. Cerrato, L. P. Reyes, C. N. Alvarado and A. M. Dietrich, Effect of PVC and iron materials on Mn(II) deposition in drinking water distribution systems, *Water Res.*, 2006, **40**(14), 2720–2726.

38 P. P. González, C. Bautista-Capetillo, A. Ruiz-Canales, J. González-Trinidad, H. E. Júnez-Ferreira, A. R. C. Rodríguez and C. O. R. Rovelo, Characterization of Scale Deposits in a Drinking Water Network in a Semi-Arid Region, *Int. J. Environ. Res. Public Health*, 2022, **19**(6), 3257.

39 R. Ketrane and C. Yahiaoui, Scale precipitation on HDPE pipe by degassing of CO₂ dissolved in water, *Aqua Water Infrastruct. Ecosyst. Soc.*, 2021, **70**(8), 1204–1216.

40 K. Aghilinasrollahabadi, M. Salehi and T. Fujiwara, Investigate the influence of microplastics weathering on their heavy metals uptake in stormwater, *J. Hazard. Mater.*, 2020, **408**, 124439.

41 K. N. Fotopoulou and H. K. Karapanagioti, Surface properties of beached plastic pellets, *Mar. Environ. Res.*, 2012, **81**, 70–77.

42 X. Huang, D. Y. Zemlyanov, S. Diaz-Amaya, M. Salehi, L. Stanciu and A. J. Whelton, Competitive heavy metal adsorption onto new and aged polyethylene under various drinking water conditions, *J. Hazard. Mater.*, 2020, **385**, 121585.

43 B. Munier and L. I. Bendell, Macro and micro plastics sorb and desorb metals and act as a point source of trace metals to coastal ecosystems, *PLoS One*, 2018, **13**(2), 1–13.

44 M. Salehi, M. Abouali, M. Wang, Z. Zhou, A. P. Nejadhashemi, J. Mitchell, S. Caskey and A. J. Whelton, Case study: Fixture water use and drinking water quality in a new residential green building, *Chemosphere*, 2018, **195**, 80–89.

45 A. J. Whelton and A. M. Dietrich, Critical considerations for the accelerated ageing of high-density polyethylene potable water materials, *Polym. Degrad. Stab.*, 2009, **94**(7), 1163–1175.

46 T. Corrales, F. Catalina, C. Peinado, N. S. Allen and E. Fontan, Photooxidative and thermal degradation of polyethylenes: interrelationship by chemiluminescence, thermal gravimetric analysis and FTIR data, *J. Photochem. Photobiol. A*, 2002, **147**(3), 213–224.

47 L. Barbeş, C. Rădulescu and C. Stihă, ATR-FTIR Spectrometry Characterization of Polymeric Materials, *Rom. Rep. Phys.*, 2014, **66**(3), 765–777.

48 M. I. Babaghayou, A. H. I. Mourad, V. Lorenzo, M. U. de la Orden, J. M. Urreaga, S. F. Chabira and M. Sebaa, Photodegradation characterization and heterogeneity evaluation of the exposed and unexposed faces of stabilized and unstabilized LDPE films, *Mater. Des.*, 2016, **111**, 279–290.

49 R. Setnescu, M. Kaci, N. Dehouche, T. Setnescu, L. Nasri and T. Zaharescu, Hydrothermal Ageing of Metallocene Polyethylene Films in Presence of Grafted Amine Stabilizers, *Arabian J. Sci. Eng.*, 2014, **40**(1), 69–80.

50 A. V. Nand, S. Ray, J. Travas-Sejdic and P. A. Kilmartin, Characterization of polyethylene terephthalate/polyaniline blends as potential antioxidant materials, *Mater. Chem. Phys.*, 2012, **134**(1), 443–450.

51 T. Luxbacher and A. P. GmbH, *The Zeta potential for solid surface analysis: a practical guide to streaming potential measurement*, Anton Paar GmbH, 2014, pp. 1-137.

52 M. Hadiuzzaman, M. Salehi and T. Fujiwara, Plastic litter fate and contaminant transport within the urban environment, photodegradation, fragmentation, and heavy metal uptake from storm runoff, *Environ. Res.*, 2022, **212**, 113183.

53 T. Ahamed, S. P. Brown and M. Salehi, Investigate the Role of Biofilm and Water Chemistry on Lead Deposition onto and Release from Polyethylene: An Implication for Potable Water Pipes, *J. Hazard. Mater.*, 2020, **400**, 123253.

54 J. López-Luna, L. E. Ramírez-Montes, S. Martínez-Vargas, A. I. Martínez, O. F. Mijangos-Ricardez, M. D. C. A. González-Chávez, R. Carrillo-González, F. A. Solís-Domínguez, M. D. C. Cuevas-Díaz and V. Vázquez-Hipólito, Linear and nonlinear kinetic and isotherm adsorption models for arsenic removal by manganese ferrite nanoparticles, *SN Appl. Sci.*, 2019, **1**(8), 1-19.

55 M. Hiles, M. Grossutti and J. R. Dutcher, Classifying formulations of crosslinked polyethylene pipe by applying machine-learning concepts to infrared spectra, *J. Polym. Sci., Part B: Polym. Phys.*, 2019, **57**(18), 1255-1262.

56 M. Grossutti, J. D'amico, J. Quintal, H. Macfarlane, A. Quirk and J. R. Dutcher, Deep Learning and Infrared Spectroscopy: Representation Learning with a β -Variational Autoencoder, *J. Phys. Chem. Lett.*, 2022, **13**, 5787-5793.

57 J. D'Amico, Tracking the Effect of Accelerated Aging on Cross-Linked Polyethylene Pipe using Fourier Transform Infrared Microscopy, *M. S. Thesis*, The University of Guelph, 2022.

58 T. L. Gorbunova, N. V. Gaevoi, K. V. Gerasimov, A. K. Chalykh and E. V. Kalugina, Effect of Chlorinated Water on Peroxide-crosslinked Polyethylene PEX-a, *Int. Polym. Sci. Technol.*, 2010, **37**(12), 59-65.

59 S. F. Chabira, M. Sebaa and C. G'sell, Influence of climatic ageing on the mechanical properties and the microstructure of low-density polyethylene films, *J. Appl. Polym. Sci.*, 2008, **110**(4), 2516-2524.

60 C. D. C. Erbetta, M. E. Silva, R. F. S. Freitas and R. G. Sousa, Accelerated aging and characterization of HDPE pin type insulators(15 kV), *Polym. Polym. Compos.*, 2021, **29**, S1641-S1648.

61 A. R. Chércoles, A. M. M. San, J. M. De La Roja and M. Gómez, Analytical characterization of polymers used in conservation and restoration by ATR-FTIR spectroscopy, *Anal. Bioanal. Chem.*, 2009, **395**(7), 2081-2096.

62 A. Martínez-Romo, R. González-Mota, J. J. Soto-Bernal and I. Rosales-Candelas, Investigating the Degradability of HDPE, LDPE, PE-BIO, and PE-OXO Films under UV-B Radiation, *J. Spectrosc.*, 2015, **2015**, 1-6.

63 N. M. Stark and L. M. Matuana, Surface chemistry changes of weathered HDPE/wood-flour composites studied by XPS and FTIR spectroscopy, *Polym. Degrad. Stab.*, 2004, **86**(1), 1-9.

64 N. M. Stark and L. M. Matuana, Characterization of weathered wood-plastic composite surfaces using FTIR spectroscopy, contact angle, and XPS, *Polym. Degrad. Stab.*, 2007, **92**(10), 1883-1890.

65 Q. Liu, Zeta Potential Measurements for Surface Modification of Plastic Substrates for Nanofluidic Biosensors, *LSU master's Theses*, Louisiana State University and Agricultural and Mechanical College, 2021, p. 5436, available from: https://digitalcommons.lsu.edu/gradschool_theses.

66 A. Asadinezhad, M. Lehocký, P. Sáha and M. Mozetič, Recent Progress in Surface Modification of Polyvinyl Chloride, *Materials*, 2012, **5**(12), 2937.

67 V. Zaporotchenko, J. Zekonyte, A. Biswas and F. Faupel, Controlled growth of nano-size metal clusters on polymers by using VPD method, *Surf. Sci.*, 2003, **532-535**, 300-305.

68 V. Zaporotchenko, T. Strunskus, K. Behnke, C. V. Bechtolsheim, A. Thran and F. Faupel, Formation of metal-polymer interfaces by metal evaporation: influence of deposition parameters and defects, *Microelectron. Eng.*, 2000, **50**(1-4), 465-471.

69 F. Zhang, Z. Hou, K. Sheng, B. Deng and L. Xie, Crystallization of calcium carbonate on polyethylene γ -radiation-grafted with acrylic acid, *J. Mater. Chem.*, 2006, **16**(13), 1215-1221.

70 A. E. Rodrigues and C. M. Silva, What's wrong with Lagergreen pseudo first order model for adsorption kinetics?, *Chem. Eng. J.*, 2016, **306**, 1138-1142.

71 Y. S. Ho and G. McKay, Pseudo-second order model for sorption processes, *Process Biochem.*, 1999, **34**(5), 451-465.

72 P. Sarin, V. L. Snoeyink, J. Bebee, W. M. Kriven and J. A. Clement, Physico-chemical characteristics of corrosion scales in old iron pipes, *Water Res.*, 2001, **35**(12), 2961-29629.

73 S. Muryanto, A. P. Bayuseno, H. Ma'mun, M. Usamah and Jotho, Calcium Carbonate Scale Formation in Pipes: Effect of Flow Rates, Temperature, and Malic Acid as Additives on the Mass and Morphology of the Scale, *Procedia Chem.*, 2014, **9**, 69-76.

74 A. A. Abokifa and P. Biswas, Modeling Soluble and Particulate Lead Release into Drinking Water from Full and Partially Replaced Lead Service Lines, *Environ. Sci. Technol.*, 2017, **51**(6), 3318-3326.

75 T. S. Gill, R. J. Knapp, S. W. Bradley and W. L. Bradley, Long term durability of crosslinked polyethylene tubing used in chlorinated hot water systems, *Plast., Rubber Compos.*, 1999, **28**(6), 309-313.

76 S. Triantafyllidou, J. Parks and M. Edwards, Lead particles in potable water, *J. - Am. Water Works Assoc.*, 2007, **99**(6), 107-117.

77 V. Javanbakht, S. A. Alavi and H. Zilouei, Mechanisms of heavy metal removal using microorganisms as biosorbent, *Water Sci. Technol.*, 2014, **69**(9), 1775-1787.